

## Evaporation Rate Effect on Starting Point of Shrinkage Stress Development During Drying Process in Solvent Cast Polymer Film

Reika Katsumata, Seisuke Ata, Keiichi Kuboyama, Toshiaki Ougizawa

Department of Organic and Polymeric Materials, Tokyo Institute of Technology, 2-12-1-S8-33, O-okayama, Meguro-ku, Tokyo 152-8552, Japan

Correspondence to: T. Ougizawa (E-mail: tougizawa@op.titech.ac.jp)

**ABSTRACT:** To reveal the effect of drying conditions on shrinkage stress existing between a film and a substrate, a polystyrene/toluene solution was coated on a glass substrate, and the volume fraction of toluene at the time when the stress starts to grow ( $\phi_S$ ) was measured at various drying temperatures and evaporation rates.  $\phi_S$  decreased with increase of drying temperature at a constant evaporation rate, while  $\phi_S$  increased with increase of evaporation rate at a constant drying temperature. From these results, it was suggested that the dominant factors affecting the starting point of stress were both the chain mobility and the measurement time-scale. Considering the two factors, the tendency of  $\phi_S$  with the drying conditions is quite similar to that of the solvent content at glass transition point, and this fact indicates a strong correlation between the starting point of stress and the glass transition of coated solution. © 2012 Wiley Periodicals, Inc. *J. Appl. Polym. Sci.* 000: 000–000, 2012

**KEYWORDS:** shrinkage stress; evaporation rate; residual stress; solvent cast; polymer film

Received 4 February 2012; accepted 31 May 2012; published online

DOI: 10.1002/app.38132

### INTRODUCTION

The solvent cast method is a way to obtain polymer films which are prepared by depositing a polymer solution onto a substrate and converting the as-deposited liquid layer into a solid. Compared with other processing methods for polymer film, such as the inflation, calendar, and melt press methods, the solvent cast films have some advantages, such as homogeneous thickness distribution, excellent transparency, free of specks, and low optical retardation. Because of these features, solvent cast films have been widely utilized in photographic, LCD, electrical, high-temperature, and other diverse applications.<sup>1</sup> However, improper drying conditions cause larger residual stress which is generated at the interface between the film and the substrate during the solvent cast process. Residual stress causes creases, interface delaminating, and folds.<sup>2</sup> To reduce residual stress, revealing its origin is desired to develop a universal theoretical strategy which can be applied to a lot of polymer solution systems. Nevertheless, optimum drying conditions to reduce residual stress have been achieved by intuition and experience in various industrial fields.

Residual stress ( $\sigma_R$ ) is the sum of the stresses which are generated in a solvent cast process. Because, in general, the solvent cast films are dried at higher temperature than the room temperature ( $T_{\text{room}}$ ), the solvent cast method consists of two processes: one is a “drying process” to evaporate the solvent at the drying temperature ( $T_{\text{dry}}$ ) and

the other is a “cooling process” to cool the film from the drying temperature to the room temperature ( $T_{\text{room}}$ ). We will define the shrinkage stress ( $\sigma_S$ ) as the stress caused by volume shrinking in the drying process at the drying temperature, and the thermal stress ( $\sigma_T$ ) as the stress caused by a difference in the coefficient of thermal expansion between a film and a substrate in the cooling process. Therefore, the residual stress is expressed as follows:<sup>3</sup>

$$\sigma_R = \sigma_S + \sigma_T \quad (1)$$

The thermal stress of polymer film on a substrate can be expressed as eq. (2):<sup>3</sup>

$$\sigma_T \approx \frac{E_{\text{film}}}{1 - \nu_{\text{film}}} (\alpha_{\text{film}} - \alpha_{\text{substrate}}) (T_{\text{room}} - T_{\text{dry}}) \quad (2)$$

where  $\alpha$ ,  $E$ , and  $\nu$  are the coefficient of thermal expansion, Young's modulus, and Poisson's ratio, respectively. Equation (2) shows that thermal stress depends on the mechanical constant, the coefficient of thermal expansion of film and substrate, and the difference between the drying temperature and the room temperature. Therefore, the choice of materials dominates the value of thermal stress, which is generated during the cooling process at a fixed drying temperature. On the other hand, shrinkage stress is too complicated to predict because it arises

during the evaporation process, which is a transient and dynamic process. This difficulty prevents us from revealing the origin of shrinkage stress.

To simplify the mechanism of shrinkage stress, we focus on its starting point based on Croll's idea.<sup>4–6</sup> Croll proposed a model focusing on the glass transition temperature ( $T_g$ ) of coatings. As a coating dries, it loses solvent and must consequently shrink.<sup>4</sup> Its thickness can contract, but the area is constrained by the substrate. There is still some solvent left after solidification, but the coating can no longer flow to satisfy the shrinkage due to the solvent loss. On the basis of this idea, Croll assumed that stress arises when the  $T_g$  of the solution equals to the drying temperature ( $T_{dry}$ ) and he evaluated the  $T_g$  of the solution with the solvent volume fraction ( $\phi_s$ ) by differential scanning calorimeter (DSC). Supposing that the volume corresponding to  $\phi_s$  shrinks isotropically, the shrinkage stress  $\sigma_s$  is evaluated by the  $\phi_s$ , the volume fraction of the solvent at  $T_g = T_{dry}$ , and retained solvent after drying ( $\phi_r$ ), shown as eq. (3).<sup>6</sup>

$$\sigma_s = \frac{E_{\text{film}}}{1 - \nu_{\text{film}}} \frac{\phi_s - \phi_r}{3(1 - \phi_r)} \quad (3)$$

It was reported that calculated  $\sigma_s$  at 23°C agreed with the experimental value measured by the cantilever method.<sup>5,6</sup> It indicates that the assumption proposed by Croll (that the starting point of shrinkage stress is the glass transition point) is considered to be reasonable to some degree. Thus, the starting point of shrinkage stress is important to investigate its origin.

However, discussions about shrinkage stress<sup>7–11</sup> have been based on the assumption, not experimental results, that stress arises at the  $T_g$ . As far as we know, there are few works<sup>12,13</sup> experimentally investigating the starting point of stress generation. In addition, although it is well known that glass transition is greatly affected by the time scale of the measurement, discussions about the influences of the evaporation rate are lacking.

In this study, the drying temperature dependence of residual, shrinkage, and thermal stress are discussed. Then we measure the starting point of shrinkage stress development by *in situ* monitoring of the stress and volume fraction of the solvent to investigate the starting point by the comparison of glass transition point of the solution. In addition, the effect of the evaporation rate on the starting point of stress development is studied.

## EXPERIMENTAL

### Materials and Sample Preparation

A polystyrene (PS;  $M_w = 420,000$ , Styron G8102, Asahi-Kasei, Japan)/toluene solution with a concentration of 12 vol % ( $\phi = 0.88$ , where  $\phi$  is the volume fraction of toluene) was prepared. At room temperature, the solution was coated on a glass substrate (24 mm × 60 mm × 0.145 mm, NEO cover glass, thickness No. 1, Matsunami Glass Ind., Japan) with a glass bar and a stainless thickness gage (0.3-mm thick) as a spacer as shown in Figure 1(a). The sample was moved to a drying chamber (inner size: 45 cm × 40 cm × 40 cm) immediately after the coating and dried following the temperature profile: the drying temperature  $T_{dry}$  was kept in a range from 20 to 80°C during the drying process and then naturally cooled down to

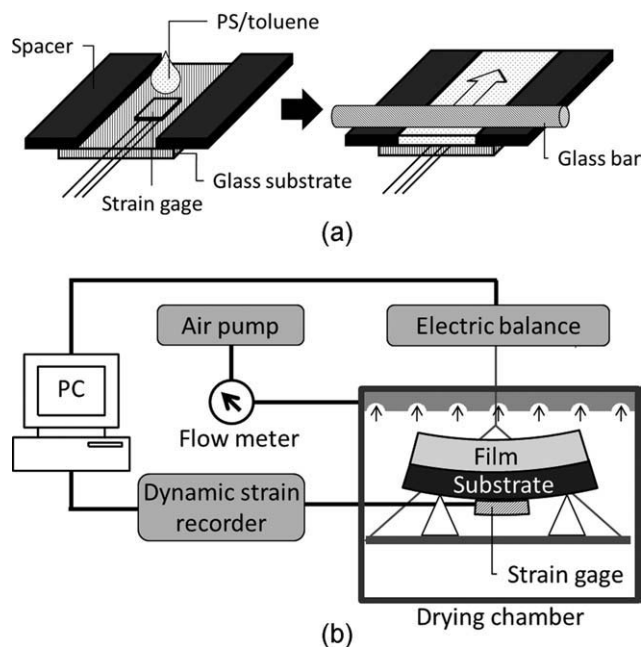


**Figure 1.** (a) Schematic diagram of applying PS/toluene solution onto a glass substrate. (b) Schematic diagram of *in situ* monitoring system of film stress and weight loss.

room temperature  $T_{\text{room}} = 20^\circ\text{C}$ . A weighing dish was hanged from the electric balance (AUW120B, Shimadzu, Japan) using a thread to monitor the solution weight during drying. We fixed the thickness of all films  $\sim 15 \mu\text{m}$ , because it is reported that film stress has no dependence on the thickness in the range from submicron to  $\sim 100 \mu\text{m}$ , in the absence of lamination or cracks.<sup>6</sup> The evaporation rate was controlled by an air pump, as shown in Figure 1(b). The flow rates of air in the drying chamber ranged from 0 to 8 L  $\text{min}^{-1}$ . The evaporation rate was evaluated from the slope of solution weight change at the beginning of the process.

### Film Stress Measurements

During the drying and cooling processes, the strain of the substrate ( $\epsilon_{\text{substrate}}$ ) was *in situ* monitored by a strain gage (3-wire system, Kyowa Electronic Instruments, Japan) which was attached to the back side of a glass substrate and connected to a dynamic strain recorder (PCD 300B, Kyowa Electronic Instruments, Japan), as illustrated in Figure 1(b). The film stress ( $\sigma$ ) was calculated from eq. (4)<sup>14</sup> and the nominal parameters of the glass substrate, where  $E_{\text{substrate}} = 71.5 \text{ GPa}$  and  $\nu_{\text{substrate}} = 0.23$ .

$$\frac{E_{\text{substrate}}}{1 - \nu_{\text{substrate}}} \epsilon_{\text{substrate}} = \sigma \quad (4)$$

### DSC Measurements

To obtain the relationship between  $\phi$  and  $T_g$ , PS/toluene solutions with various toluene volume fractions ( $\phi = 0, 0.0411, 0.117, \text{ and } 0.306$ ) were prepared in sealed DSC pans. After sealing, the specimens were annealed at 30°C for >3 days to disperse the toluene homogeneously into the PS. DSC measurement was performed at various heating rates ( $q = 5, 10, \text{ and } 20^\circ\text{C min}^{-1}$ ).  $T_g$  was evaluated as onset value in the heating process.

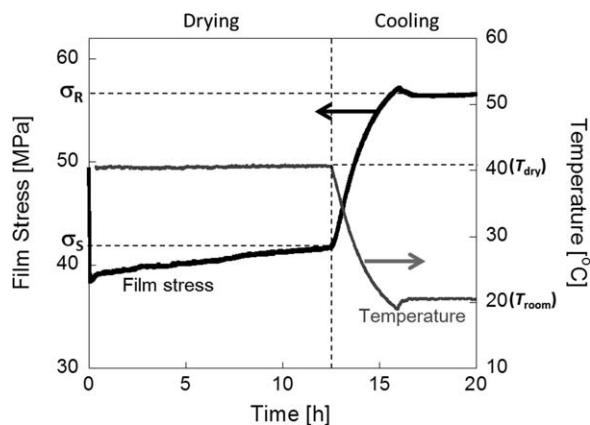


**Figure 2.** Typical profile of film stress and temperature during solvent cast process at  $T_{\text{dry}} = 40^\circ\text{C}$ .

## RESULTS AND DISCUSSION

### Drying Temperature Dependence of Residual Stress, Thermal Stress, and Shrinkage Stress

Figure 2 shows the time dependence of the film stress during the drying process ( $T_{\text{dry}} = 40^\circ\text{C}$ ) and the cooling process ( $T_{\text{dry}} = 40^\circ\text{C} \rightarrow T_{\text{room}} = 20^\circ\text{C}$ ). Thermal stress ( $\sigma_T$ ) was estimated as  $(\sigma_R - \sigma_S)$  from eq. (1). Neither lamination nor cracks were observed in the sample after these processes. We conducted the same experiment as Figure 2 with different  $T_{\text{dry}} = 20\text{--}80^\circ\text{C}$ . In Figure 3, residual stress, thermal stress, and shrinkage stress as a function of  $T_{\text{dry}}$  are plotted for PS film prepared from the PS/toluene solution on a glass substrate. The residual stress has a minimum value at  $T_{\text{dry}} \approx 50^\circ\text{C}$  and it means that  $50^\circ\text{C}$  is approximately the optimum temperature to minimize the residual stress in this system. As shown in eq. (1), residual stress can be divided into thermal stress and shrinkage stress. In Figure 3, the thermal stress linearly increases with  $T_{\text{dry}}$ , while the shrink-

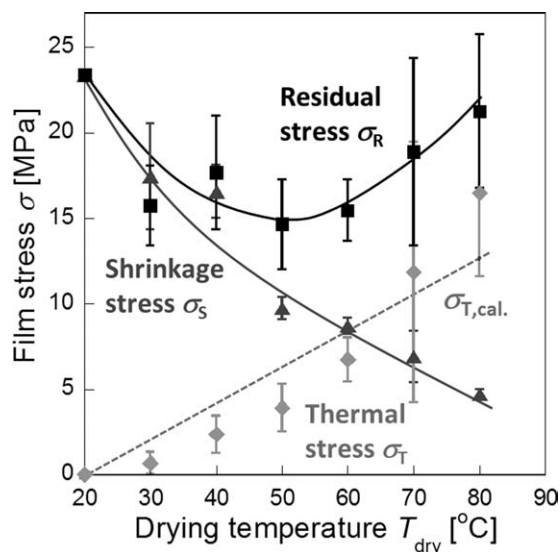


**Figure 3.** Residual stress  $\sigma_R$  (square), thermal stress  $\sigma_T$  (rhombus), and shrinkage stress  $\sigma_S$  (triangle) as functions of drying temperature ( $T_{\text{dry}}$ ). Broken line is calculated thermal stress ( $\sigma_{T,\text{cal.}}$ ).

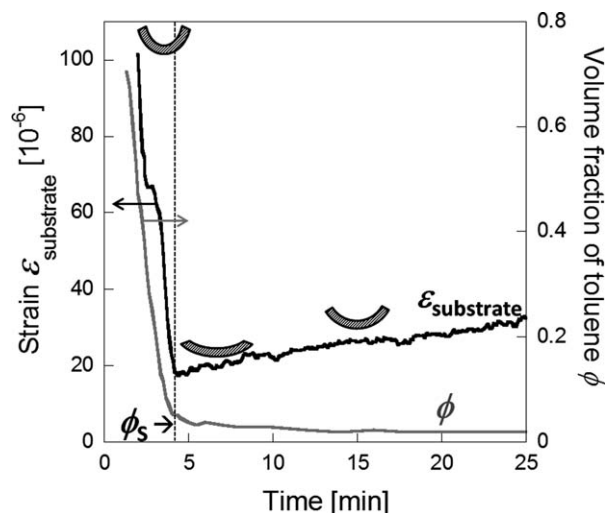


**Figure 4.** Time variation of strain of substrate ( $\epsilon_{\text{substrate}}$ ) and volume fraction of toluene ( $\phi$ ) at  $T_{\text{dry}} = 70^\circ\text{C}$ . The inserted diagram represents the schematic lateral view of the substrate.

age stress decreases monotonically. This indicates that the minimum value of residual stress is determined by competition between the other two stresses. By assigning the parameters of the film and the substrate,  $E_{\text{film}} = 1.64\text{ GPa}$ ,  $\nu_{\text{film}} = 0.33$ ,<sup>15</sup>  $\alpha_{\text{film}} = 9.15 \times 10^{-5}\text{ K}^{-1}$  and  $\alpha_{\text{substrate}} = 7.2 \times 10^{-6}\text{ K}^{-1}$  respectively into eq. (2), the thermal stress is calculated and shown by a broken line as  $\sigma_{T,\text{cal.}}$  in Figure 3.  $E_{\text{film}}$  is determined by tensile test and  $\alpha_{\text{film}}$  by pressure–volume–temperature data.<sup>16</sup> We can see that  $\sigma_{T,\text{cal.}}$  almost agrees with  $\sigma_T$  which means that eq. (2) describes thermal stress well and that thermal stress is easy to predict. In regard to residual stress being the sum of thermal stress and shrinkage stress, revealing the mechanism of shrinkage stress is necessary to reduce residual stress. However, the mechanism of shrinkage stress is very complicated because it is generated during solvent evaporation, which is a transient and dynamic process. Therefore, we simplify the phenomenon by focusing on the starting points of shrinkage stress.

### Starting Point of Shrinkage Stress Development

The starting point of shrinkage stress was evaluated by *in situ* monitoring of the strain of substrate ( $\epsilon_{\text{substrate}}$ ) and weight of the PS/toluene solution. Figure 4 shows the time variation of  $\epsilon_{\text{substrate}}$  at  $T_{\text{dry}} = 70^\circ\text{C}$ . The inserted diagram represents the schematic lateral view of the substrate to show degree of the substrate deformation. In the beginning of the process, the  $\epsilon_{\text{substrate}}$  decreases but starts increasing around  $t = 4\text{ min}$ . During the initial stage of the process, the glass substrate bends by the weight of the solution on the substrate and the bending is detected as the strain. As the solvent evaporates, the  $\epsilon_{\text{substrate}}$  decreases monotonically with time by solvent loss. If shrinkage stress is not generated, the strain should monotonically decrease with time, but generation of shrinkage stress makes the strain increase. Thus, the time when  $\epsilon_{\text{substrate}}$  starts increasing is considered to be the starting point of the development of the shrinkage stress and we define  $\phi_S$  as the volume fraction of toluene at the starting point of shrinkage stress.

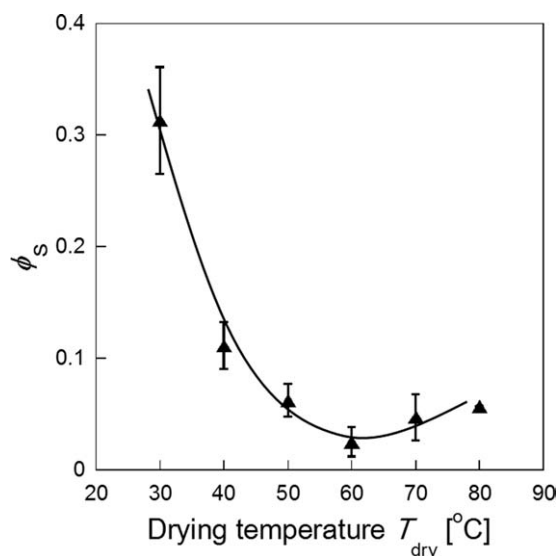


**Figure 5.** Volume fraction of toluene at starting point of shrinkage stress ( $\phi_S$ ) as a function of  $T_{\text{dry}}$ .

measured at various  $T_{\text{dry}}$  as shown in Figure 5.  $\phi_S$  decreases until  $T_{\text{dry}} = 60^\circ\text{C}$  and starts increasing at a higher  $T_{\text{dry}}$ .

We investigated whether the starting point of shrinkage stress is the glass transition point of the solution or not based on an idea shown in Figure 6. Figure 6 is a schematic diagram which shows the relationship between temperature and volume fraction of solvent at the glass transition point. In general,  $T_g$  of a polymer solution decreases with an increase in solvent content by a plasticizing effect,<sup>17</sup> which makes the polymer softer by adding solvent, as shown in Figure 6. As a polymer solution is dried at a constant drying temperature  $T_0$ , the volume fraction of the solvent ( $\phi$ ) decreases following the (a) route and the solution transfers to glass at  $\phi_0$ . If the starting point of shrinkage stress is the glass transition point,  $\phi_0$  should be equal to  $\phi_S$  at  $T_{\text{dry}} = T_0$ . Whereas, if we con-

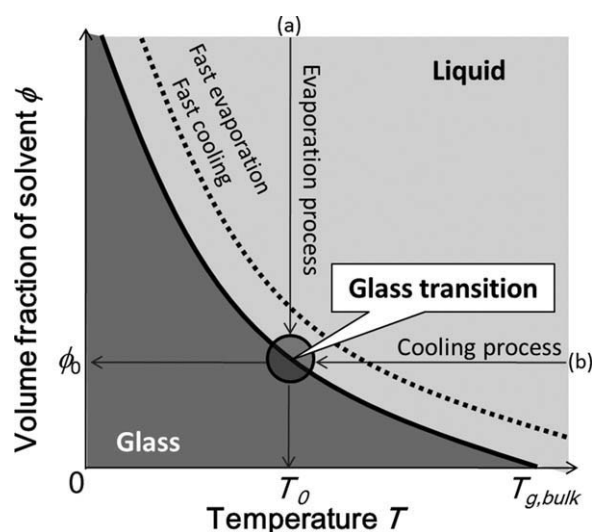


**Figure 6.** Conceptual diagram of relationship between  $T_g$  and  $\phi$ . (a) Route represents the evaporation process and (b) route the cooling process.

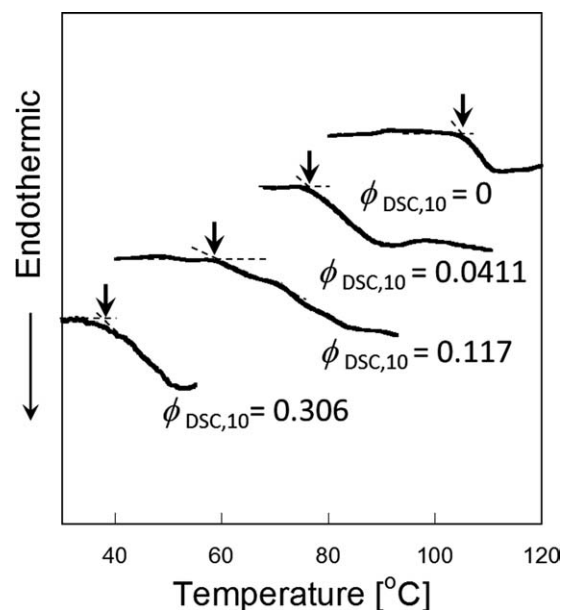


**Figure 7.** DSC thermograms of the solution with different solvent content measured with heating rate of  $10^\circ\text{C min}^{-1}$ .

sider this glass transition from the temperature axis, the (b) route can be regarded as the cooling process of the solution with a certain volume fraction,  $\phi_0$ . When the temperature decreases following the (b) route, the solution with  $\phi_0$  transfers to glass at  $T_0 (= T_g)$  because of the reduction in molecular mobility by a decrease in temperature. For these reasons, comparing  $\phi_{\text{DSC},q}$  measured by DSC following the (b) route with  $\phi_S$  measured by *in situ* monitoring of the stress following the (a) route can be a way to investigate whether the starting point of stress development is the glass transition point of the solution or not.

To confirm this, we evaluated the  $T_g$  of polymer solutions with various  $\phi$ . Figure 7 shows the DSC thermograms of PS/toluene solution with different  $\phi_{\text{DSC},q}$  measured with a heating rate of  $q = 10^\circ\text{C min}^{-1}$  and each arrow indicates  $T_g$ .  $T_g$  as a function of  $\phi_{\text{DSC},10}$  is plotted in Figure 8. If shrinkage stress is generated at  $T_g (= T_{\text{dry}})$ ,  $\phi_{\text{DSC},q}$  should be equal to the volume fraction of toluene at the starting point of shrinkage stress ( $\phi_S$ ). To compare  $\phi_S$  with  $\phi_{\text{DSC},q}$  we interchanged the axis of the plot in Figure 8 between the volume fraction of toluene and  $T_g$  and then plotted the  $\phi_{\text{DSC},q}$  as a function of  $T_{\text{dry}}$  in Figure 9.  $T_g$  measurement of the solution was carried out with  $q = 5, 10, 20^\circ\text{C min}^{-1}$  to concern the effect of the heating rate.<sup>18–21</sup> The  $\phi_S$  shown in Figure 5 is also plotted to compare it with  $\phi_{\text{DSC},q}$ . In low temperature region, both  $\phi_S$  and  $\phi_{\text{DSC},q}$  decrease with  $T_{\text{dry}}$ , which can be regarded as a similar behavior between  $\phi_S$  and  $\phi_{\text{DSC},q}$  despite the difference in their absolute value. On the other hand, in high temperature region,  $\phi_S$  increases with  $T_{\text{dry}}$  while  $\phi_{\text{DSC},q}$  decreases, that is,  $\phi_S$  was not in agreement with  $\phi_{\text{DSC},q}$  in this region. This difference of behavior cannot be explained by the increase of chain mobility with increase in temperature. Concerning only temperature, chain mobility will get larger with temperature increasing and it means the coated solution solidifies with less solvent content at higher temperature. Therefore,  $\phi_S$  is expected to monotonically decrease with  $T_{\text{dry}}$ . The other factor affecting the starting point is evaporation rate, because glass transition strongly

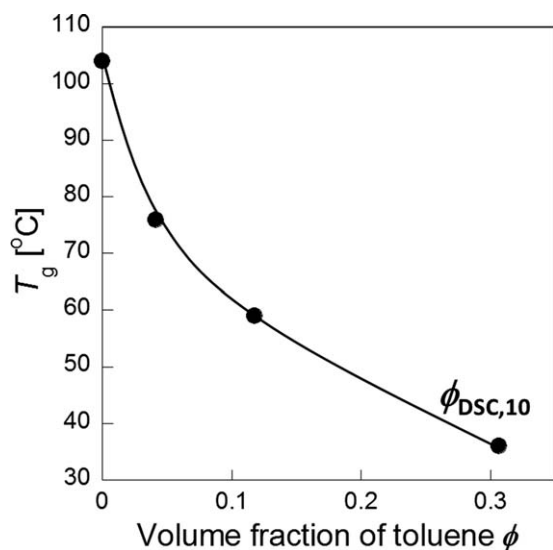


**Figure 8.**  $T_g$  of polystyrene/toluene solution as a function of  $\phi_{DSC,10}$ .  $T_g$  was measured by DSC with a heating rate of  $q = 10^\circ\text{C min}^{-1}$ .

depends on the measurement time-scales. The  $T_{dry}$  dependence of the evaporation rate is shown in Figure 10. The evaporation rate increases with  $T_{dry}$ , which means that the measurement time-scale decreases with  $T_{dry}$ .

#### Factors Affecting the Starting Point of Shrinkage Stress

To separate the influence of the evaporation rate from the  $T_{dry}$ , we measured  $\phi_S$  at a constant temperature of  $20^\circ\text{C}$  with various evaporation rates using the apparatus shown in Figure 1(b). Figure 11 illustrates the evaporation rate dependence of  $\phi_S$ , and  $\phi_S$  increases with the evaporation rate. This tendency denotes that shrinkage stress is generated at a larger solvent content with a faster evaporation. Increasing  $\phi_S$  by the evaporation rate can also be confirmed

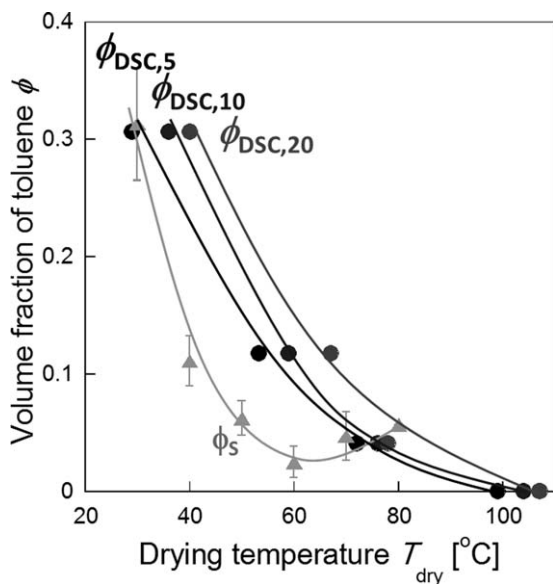


**Figure 9.**  $\phi_S$  (triangle) and  $\phi_{DSC,q}$  (circle) as functions of  $T_{dry}$ , measured with  $q = 5, 10, 20^\circ\text{C min}^{-1}$ .

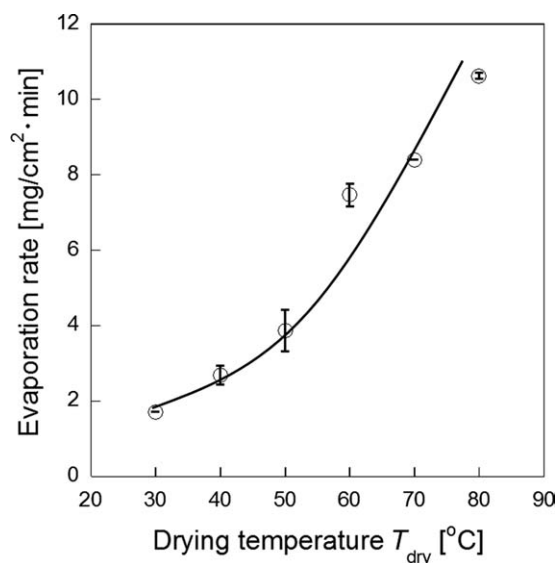


**Figure 10.**  $T_{dry}$  dependence of evaporation rate.

by DSC measurement. Generally, a higher  $T_g$  is observed when the  $T_g$  is measured with a larger heating/cooling rate because glass transition depends on the measurement time-scale.<sup>18–21</sup> In the cases that a polymer solution is heated/cooled rapidly and solvent evaporates rapidly, the  $\phi - T_g$  curve in Figure 6 moves upward, shown as a broken line. In other words, the influence of the evaporation rates on  $\phi_S$  is considered to correspond to that of the heating/cooling rate on glass transition in terms of measurement time-scale. From these discussions, it was found that  $\phi_S$  increases with the evaporation rate at a constant  $T_{dry}$  while  $\phi_S$  decreases with  $T_{dry}$  at a constant evaporation rate.

The increase of  $\phi_S$  at high  $T_{dry}$  in Figure 9 can be explained by concerning the increase of  $\phi_S$  with increase of evaporation rate. The increase of  $\phi_S$  should be the result from higher evaporation rate at the higher  $T_{dry}$  as shown in Figure 10. This can also be confirmed from the view point of the correspondence between the evaporation

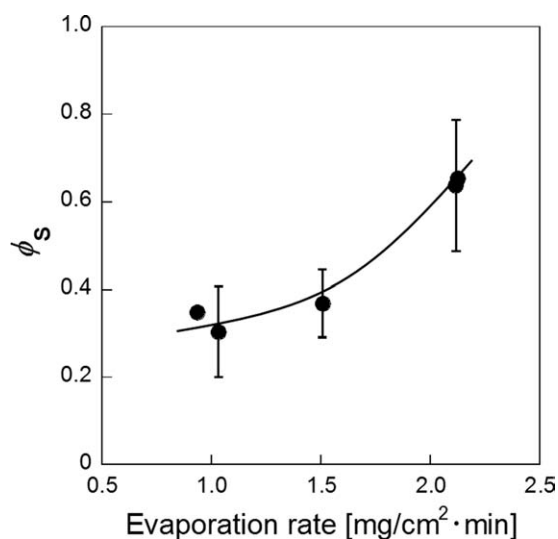


**Figure 11.**  $\phi_S$  as a function of evaporation rate at  $T_{dry} = 20^\circ\text{C}$ .

rate and the heating rate  $q$ . In Figure 9, we can see that  $\phi_{\text{DSC},q}$  increases with increase of  $q$ , i.e., the decrease of measurement time-scale. For instance,  $\phi_S$  is close to  $\phi_{\text{DSC},10}$  at low  $T_{\text{dry}}$ , while  $\phi_S$  is close to  $\phi_{\text{DSC},20}$  at high  $T_{\text{dry}}$ . These discussions show that the change of  $\phi_S$  with  $T_{\text{dry}}$  is similar to that of glass transition, and therefore, it can be considered that the starting point of shrinkage stress strongly correlate with glass transition of coated solution. However, there are some important quantitative differences between the two curves at higher temperature, and further investigation would be warranted.

## CONCLUSIONS

The starting point of shrinkage stress development was studied through *in situ* monitoring of shrinkage stress and toluene content in a PS solution during the drying process. Under various drying temperatures and evaporation rates, we compared the volume fraction of toluene at the starting point of the shrinkage stress ( $\phi_S$ ) with that at  $T_g$  of the PS solution measured by DSC with various heating rate  $q$  ( $\phi_{\text{DSC},q}$ ). The experiments showed that  $\phi_S$  decreased with temperature due to increase of chain mobility at a constant evaporation rate, while  $\phi_S$  increases with evaporation rate, because it was observed in short measurement time-scale at a constant drying temperature. Therefore, it was revealed that the  $\phi_S$  under a certain drying condition was determined in the balance between the chain mobility and the measurement time-scale. In the same manner,  $\phi_{\text{DSC},q}$  decreased with  $T_{\text{dry}}$  at a constant  $q$ , while  $\phi_{\text{DSC},q}$  increased with  $q$  at a constant  $T_{\text{dry}}$ . The increase of both the evaporation rate and the  $q$  corresponded to the decrease of measurement time-scale. From these results, it was shown that the starting point of shrinkage stress had a strong correlation with the glass transition of coated solution. The results of this study could have important implications for revealing the mechanism of the evaporation rate dependence of shrinkage stress. However, we would like to note that further investigation is needed in terms of the relationship between volume fraction of solvent at the starting point of shrinkage stress and the shrinkage stress after finishing drying.

## REFERENCES

1. Siemann, U. *Progr. Colloid Polym. Sci.* **2005**, *130*, 1.
2. Ree, M.; Shin, T.; Park, Y.; Kim, S.; Woo, S. H.; Cho, C. K.; Park, C. E. *J. Polym. Sci. B Polym. Phys.* **1998**, *36*, 1261.
3. Ohring, M. *The Materials Science of Thin Films*; Academic Press: New York, **2002**.
4. Croll, S. G. *J. Coating Technol.* **1978**, *50*, 33.
5. Croll, S. G. *J. Coating Technol.* **1979**, *51*, 64.
6. Croll, S. G. *J. Appl. Polym. Sci.* **1979**, *23*, 847.
7. Payne, J. A.; McCormick, A. V.; Francis, L. F. *J. Appl. Polym. Sci.* **1999**, *73*, 553.
8. Reiter, G. *Eur. Polym. J. E.* **2001**, *28*, 25.
9. Chung, J. Y.; Chastek, T. Q.; Fasolka, M. J.; Ro, H. W.; Stafford, C. M. *ACS Nano.* **2009**, *3*, 844.
10. Reiter, G.; Hamieh, M.; Damman, P.; Sclavons, S.; Gabriele, S.; Vilmin, T.; Raphaël, E. *Nat. Mater.* **2005**, *4*, 754.
11. Ree, M.; Chu, C. W.; Goldberg, M. J. *J. Appl. Phys.* **1994**, *75*, 1410.
12. Inoue, Y.; Kobatake, Y. *Kolloid Z.* **1958**, *159*, 18.
13. Vaessen, D. M.; McCormick, A. V.; Francis, L. F. *Polymer* **2002**, *43*, 2267.
14. Chiu, C. *J. Am. Ceram. Soc.* **1990**, *73*, 7.
15. Brandup, J.; Immergut, E.; Grulke, E. *Polymer Handbook*, 4th ed.; Wiley-Interscience: New York, **1999**.
16. Hagiwara, K.; Ougizawa, T.; Inoue, T.; Hirata, K.; Kobayashi, Y. *Radiat. Phys. Chem.* **2000**, *58*, 525.
17. Chow, T. S. *Macromolecules* **1980**, *13*, 362.
18. Moynihan, C. T.; Easteal, A. J.; Wilder, J.; Tucker, J. *J. Phys. Chem.* **1974**, *78*, 2673.
19. Crichton, S. *J. Non-Cryst. Solids* **1988**, *99*, 413.
20. Simatos, D.; Blond, G.; Roudaut, G.; Champion, D.; Perez, J.; Faivre, A. L. *J. Therm. Anal.* **1996**, *47*, 1419.
21. Montserrat, S.; Calventus, Y.; Hutchinson, J. *Polymer* **2005**, *46*, 12181.